

Upper limits on supermassive black holes from STIS archival data

A. Beifiori¹, E.M. Corsini¹, E. Dalla Bontà¹, A. Pizzella¹, L. Coccato³, M. Sarzi², and F. Bertola¹

¹ Dipartimento di Astronomia, Padova, Italy, ² Centre for Astrophysics Research, Hatfield, UK, ³ Kapteyn Astronomical Institute, Groningen, The Netherlands

ABSTRACT

The growth of supermassive black holes (SBHs) appears to be closely linked with the formation of spheroids. From the observational point of view there is a pressing need to acquire better M_{BH} statistics since the existing samples are preferentially weighted toward early-type galaxies with very massive SBHs. With this motivation we started a project aimed at measuring upper limits of the mass of the SBHs that can be present in the centers of all the nearby galaxies ($D < 100$ Mpc) for which STIS/G750M spectra are available in the HST archive. These limits will be derived from the modeling of the central emission-line widths ([NII]6548,6583Å, H α and [SII]6716,6730 Å) observed over an aperture of $\sim 0.1''$ ($R < 50$ pc). In this poster we present our preliminary results about a subsample of 20 bulges of early-type disk galaxies (S0–Sb) within 20 Mpc.

1. INTRODUCTION

The census of supermassive black holes (SBHs) is large enough to probe the links between mass of SBHs and the global properties of the host galaxies, namely the mass and luminosity of the host spheroid, the central velocity dispersion, the light concentration, and the mass of the dark halo (see Ferrarese & Ford 2005, SSRv, 116, 532, for a review). However, accurate measurements of SBH masses are available for few tens of galaxies and the addition of new determinations is highly desirable.

To this purpose we started a project aimed at measuring upper limits on the mass of the SBHs that can be present in the centers of all the nearby galaxies ($D < 100$ Mpc) for which STIS/G750M spectra are available in the HST archive. We retrieved data for 212 galaxies spanning over all the morphological types (18% Es, 41% S0s, 62% spirals, 1% irregulars). This will extend previous works by Sarzi et al. (2002, ApJ, 567, 237) and Verdoes-Klein et al. (2006, astro-ph/0601023).

2. SAMPLE SELECTION AND ARCHIVAL DATA

Here we analyze a subsample of 23 galaxies. They have been selected to be S0–Sb within 20 Mpc, and a central stellar velocity dispersion (σ_*) available in literature. All the galaxies were observed as part of the SUNNS project (PI: H.-W. Rix, GO-7361) except for NGC 4435 (Coccatto et al. 2006, MNRAS, 336, 1050). Their basic properties are listed in Table 1.

The STIS/G750M spectra were obtained with the $0.2'' \times 52''$ slit crossing either the galaxy nucleus along a random position angle (SUNNS) or along the galaxy major axis (NGC 4435). The observed spectral region includes the [NII]6548,6583Å, H α , and [SII]6716,6730Å emission lines.

Object name (1)	Hubble Type (2)	Spectral class (3)	M_B^g [mag] (4)	P.A. [°] (5)	i [°] (6)	D [Mpc] (7)	σ_* [km s ⁻¹] (8)	σ_{gas} [km s ⁻¹] (9)	M_{BH} [$10^7 M_{\text{sun}}$] (10)	M_{BH} [$10^7 M_{\text{sun}}$] (11)
NGC 2787	SB0/a	L1.9	11.04	117	49.8	13.0	210 ± 23	210 ± 7	13.4	18.4
NGC 3351	SBb(r)	H	10.71	13	47.5	8.1	101 ± 16	51 ± 2	0.02	0.006
NGC 3368	Sab(s)	L2	10.25	5	46.2	8.1	135 ± 10	102 ± 4	2.8	3.0
NGC 3992	SBb(rs)	T2:	10.03	68	51.9	17.0	140 ± 20	105 ± 3	4.7	5.5
NGC 4143	SO[1](s)/Sa	L1.9	15.67	144	50.9	17.0	270 ± 12	215 ± 3	8.8	19.1
NGC 4203	SO[2](l)	L1.9	15.38	10	21.0	17.0	124 ± 16	154 ± 5	7.5	8.4
NGC 4245	SBa(s)	H	15.92		40.7	12.2		107 ± 28	2.9	3.1
NGC 4314	SBa(rs)pec	L2	15.05		26.9	13.2	119 ± 9	64 ± 5	0.9	0.5
NGC 4321	Sc(s)	T2	13.75	30	31.7	16.8	83 ± 12	75 ± 1	1.3	1.8
NGC 4435	SB0[1](7)	T2/H:	15.40	13	43.6	16.0	165 ± 13	103 ± 4	3.0	3.4
NGC 4450	Sab pec	L1.9	14.52	175	42.2	16.8	130 ± 17	162 ± 3	14.1	15.5
NGC 4459	SO[3](s)	T2:	14.98	110	40.7	16.8	189 ± 21	191 ± 8	14.4	18.1
NGC 4477	SB0[1/2]/SBa	S2	15.07	15	24.2	16.8	156 ± 12	117 ± 2	5.8	7.2
NGC 4501	Sbc(s)	S2	13.63	140	57.5	16.8	151 ± 17	96 ± 1	4.2	5.0
NGC 4548	SBb(rs)	L2	14.56	150	37.4	16.8	85 ± 9	83 ± 2	2.6	3.0
NGC 4596	SBa	L2:	15.27	135	42.2	16.8	154 ± 5	165 ± 11	6.8	12.1
NGC 4698	Sa	S2	15.01	170	43.6	16.8	134 ± 6	98 ± 2	4.3	5.7
NGC 4800	Sb(rs)	H	15.55	25	42.2	15.2	112 ± 2	96 ± 10	3.0	3.6

Table 1. Observed and derived properties for the sample galaxies

3. DATA ANALYSIS

Basic data reduction, wavelength and flux calibration were performed with the STIS pipeline, which we implemented to clean the cosmic rays and hot pixels. For each galaxy we obtained the nuclear spectrum by extracting a $0.25''$ -wide (< 25 pc) aperture centered on the continuum peak.

The ionized-gas velocity dispersion (σ_{gas}) was measured by the fitting Gaussians with the same width and velocity to the narrow component of the [NII] and [SII] emission lines. The H α line and broad components were fitted with additional Gaussians. Fit results are shown in Figure 1. NGC 278, NGC 3489, NGC 3892, NGC 4380 and NGC 5055 were excluded from further analysis due the poor signal-to-noise ratio of their spectra. NGC 4245 and NGC 4314 were not measured by Sarzi et al. (2002).

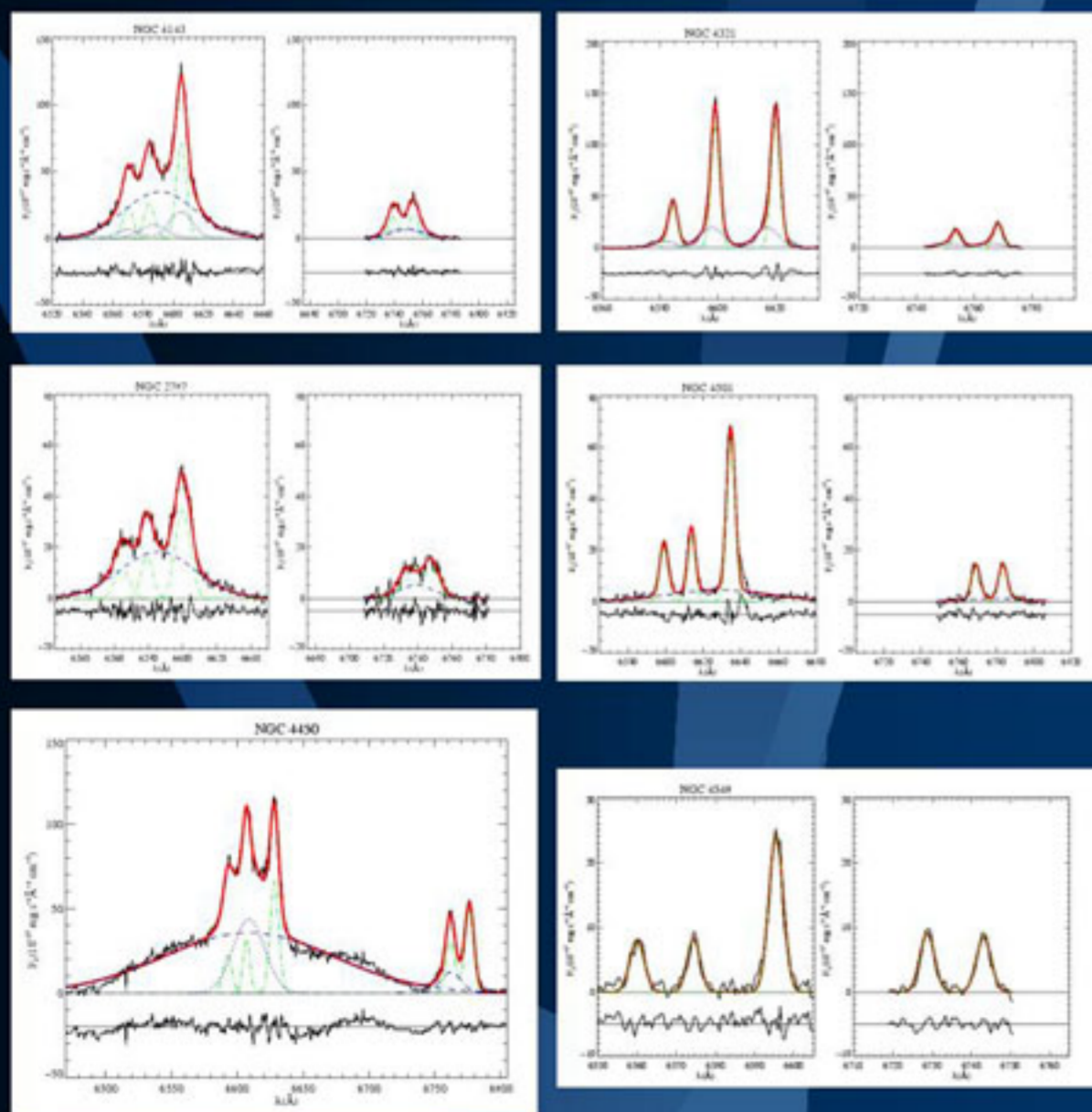


Figure 1. For some of the sample galaxies we show the continuum-subtracted spectra (black line) in the H α + [NII] (left panel) and [SII] (right panel) regions, plotted with Gaussian model components (green and blue lines for narrow and broad components, respectively), and the reconstructed blend (red line). In each panel the residuals have been offset for better visibility.

4. KEPLERIAN DISK MODEL

We assumed that the ionized gas resides in a thin disk and moves onto circular orbits at the local circular velocity. This is dictated by the gravitational influence of the putative SBH. To derive the upper limits on M_{BH} we first built the gaseous velocity field and projected it onto the sky plane according to the disk orientation. Then we observed it by simulating the actual setup of STIS and effects related to the STIS PSF, slit width and the charge bleeding as done by Coccatto et al. (2006). Including the mass contribution of the stellar component would lead to tighter upper limits on M_{BH} .

We have no information on the orientation of the gaseous disk within the central aperture. For this pilot project we assumed that the disk is nearly face on ($i=32^\circ$) and the slit is placed along its major axis. We derived the intrinsic flux radial profile of the gaseous disk by fitting either an exponential or a Gaussian function to the narrow emission-line fluxes taking into account for disk inclination and STIS PSF. In Figure 2 we show the model line profile as a function of M_{BH} and disk orientation.

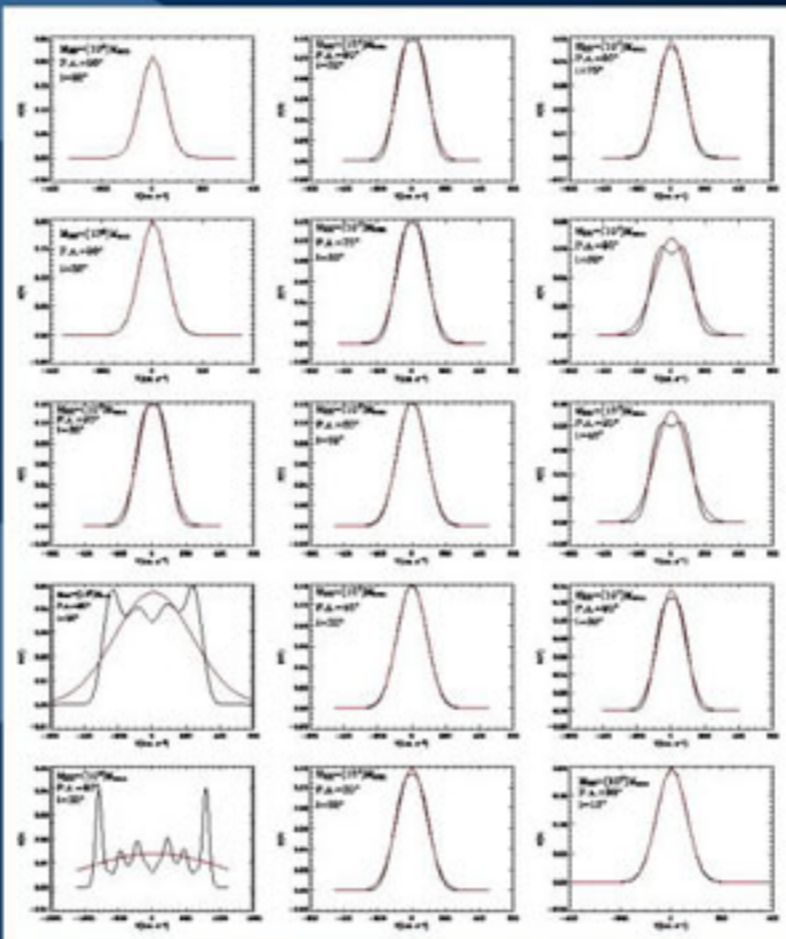


Figure 2. Line profile of the [NII]6583Å emission line (black line) with its Gaussian model (red line) as a function of M_{BH} (left column, for 10° , 10° , 10° , 10° , $10^\circ M_{\text{sun}}$ with $i=32^\circ$ and slit along the disk major axis), slit location (middle column, for a slit along the major axis, and at an intermediate angle of 15° , 30° , 45° , and 60° with $i=32^\circ$ and $M_{\text{BH}}=10^7 M_{\text{sun}}$) and inclination (right column, for 75° , 60° , 45° , 30° , and 15° with $M_{\text{BH}}=10^7 M_{\text{sun}}$ and the slit along the major axis)

5. RESULTS

The resulting upper limits on M_{BH} are given in Table 1 for both the exponential (col. 10) and Gaussian (col. 11) flux profile. Figure 3 shows they are consistent within a factor 2 with those derived by Sarzi et al. (2002) for the SUNNS sample. Our limit on the mass of the central SBH of NGC 4435 is ~ 4 times larger than that found by Coccatto et al. (2006) by modeling the resolved ionized-gas kinematics measured along the major axis and two offset parallel positions.

Figure 4 shows that three of the upper limits we derived lie below the scatter of the $M_{\text{BH}}-\sigma_*$ relation (Ferrarese & Ford 2005) and therefore are not consistent with it. (NGC 3351 $\sigma_*=101$ km/s, NGC 4314 $\sigma_*=119$ km/s, NGC 4143 $\sigma_*=270$ km/s)

This approach is potentially applicable to all the galaxies for which we retrieved a STIS/G750M spectrum. This will allow to increase the statistical significance of the relationships between M_{BH} and galaxy properties and identify peculiar cases worthy of further investigations.

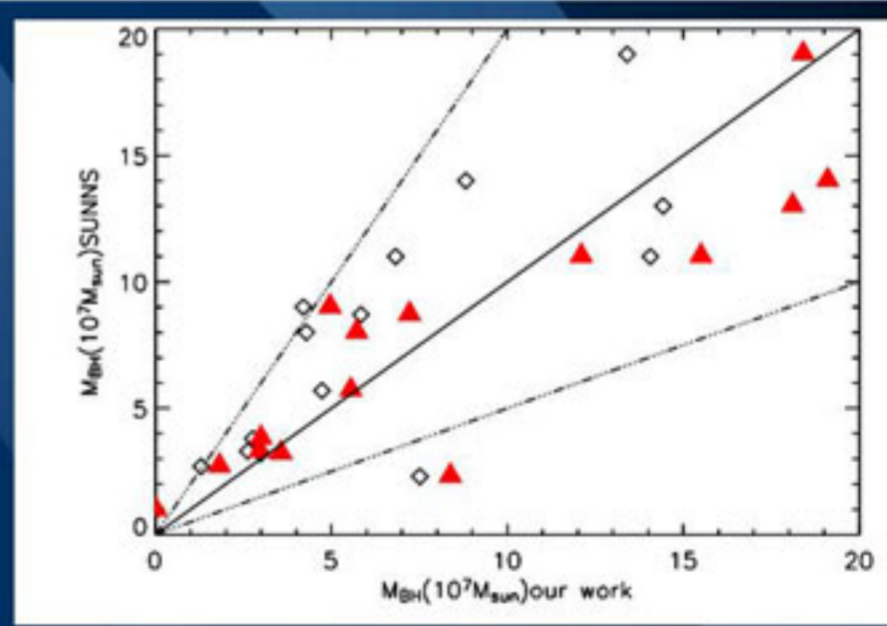


Figure 3. Comparison between our upper limits on the mass of SBHs of the SUNNS galaxies and those derived by Sarzi et al. (2002). Dotted lines mark the region where the difference between our and their estimates are smaller than a factor 2. Red triangles and open diamonds correspond to the values we derived by assuming for the intrinsic flux of the gaseous disk an exponential and Gaussian profile, respectively. Sarzi et al. (2002) adopted a Gaussian profile.

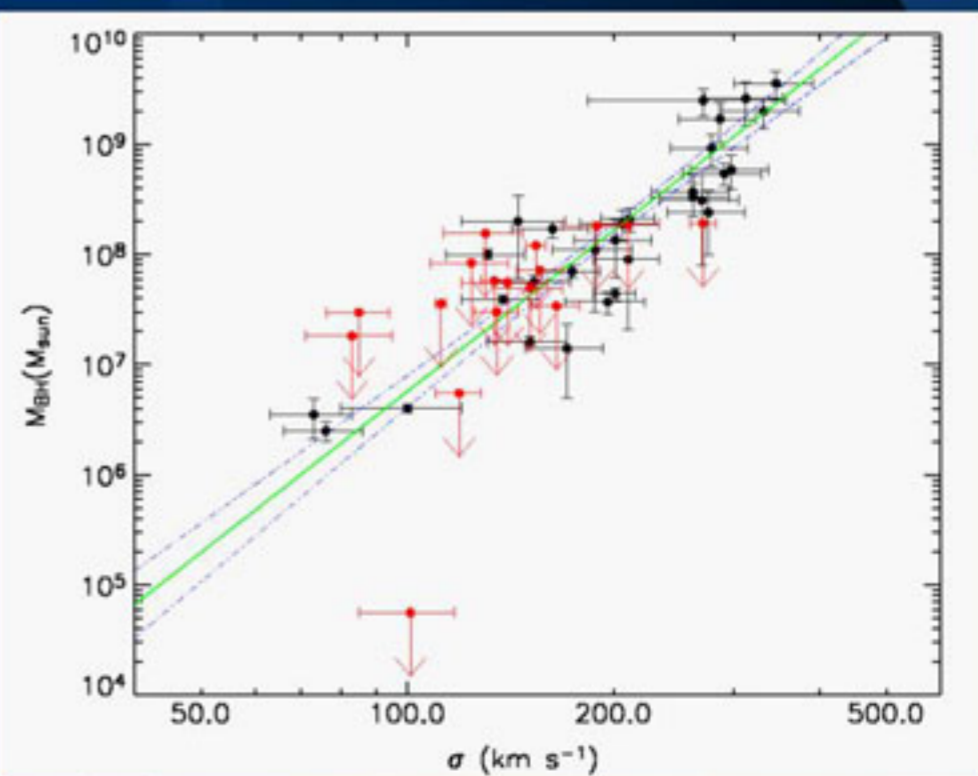


Figure 4. Comparison between our M_{BH} upper limits (red dots) and the $M_{\text{BH}}-\sigma_*$ relation by Ferrarese & Ford (2005, green continuous line). Black dots correspond to the galaxies with an accreting BH mass for which the sphere of influence was resolved by the data. The blue dashed line is the absolute scatter. The smallest upper limits corresponds to NGC 3351.